

Modeling benzene permeation through drinking water high density polyethylene (HDPE) pipes

Feng Mao, Say Kee Ong and James A. Gaunt

ABSTRACT

Organic compounds such as benzene, toluene, ethyl benzene and *o*-, *m*-, and *p*-xylene from contaminated soil and groundwater may permeate through thermoplastic pipes which are used for the conveyance of drinking water in water distribution systems. In this study, permeation parameters of benzene in 25 mm (1 inch) standard inside dimension ratio (SIDR) 9 high density polyethylene (HDPE) pipes were estimated by fitting the measured data to a permeation model based on a combination of equilibrium partitioning and Fick's diffusion. For bulk concentrations between 6.0 and 67.5 mg/L in soil pore water, the concentration-dependent diffusion coefficients of benzene were found to range from 2.0×10^{-9} to 2.8×10^{-9} cm²/s while the solubility coefficient was determined to be 23.7. The simulated permeation curves of benzene for SIDR 9 and SIDR 7 series of HDPE pipes indicated that small diameter pipes were more vulnerable to permeation of benzene than large diameter pipes, and the breakthrough of benzene into the HDPE pipe was retarded and the corresponding permeation flux decreased with an increase of the pipe thickness. HDPE pipes exposed to an instantaneous plume exhibited distinguishable permeation characteristics from those exposed to a continuous source with a constant input. The properties of aquifer such as dispersion coefficients (D_L) also influenced the permeation behavior of benzene through HDPE pipes.

Key words | benzene, diffusion, drinking water, permeability, plastic pipes, polyethylene

Feng Mao (corresponding author)
Arizona Department of Environmental Quality,
1110 West Washington Street,
Phoenix,
AZ 85007,
USA
E-mail: mf8@azdeq.gov

Say Kee Ong
James A. Gaunt
Department of Civil, Construction and
Environmental Engineering,
Iowa State University,
Ames,
IA 50010,
USA

INTRODUCTION

Spills and leaks of petroleum hydrocarbons such as gasoline, diesel, and motor oils have caused widespread subsurface contamination by toxic and water soluble compounds such as benzene, toluene, ethyl benzene and *o*-, *m*-, and *p*-xylene (BTEX). These pollutants from contaminated soil and groundwater may permeate through thermoplastic pipes and gaskets which are used for the conveyance of drinking water in water distribution systems, resulting in drinking water contamination (Thompson & Jenkins 1987; US EPA 2002; Ong *et al.* 2008). To evaluate the contamination of potable water due to chemical permeation, many studies have been conducted to investigate the permeation of organic contaminants through polybutylene (PB) pipes (Holsen *et al.* 1991; Park *et al.* 1991), polyethylene (PE) pipes (Holsen *et al.* 1991; Mao *et al.* 2010), polyvinyl chloride pipes (Berens 1985; Vonk 1985;

Mao *et al.* 2009, 2011a) as well as gaskets used for joining and sealing two lengths of plastic pipes (Glaza & Park 1992; Mao *et al.* 2011b; Cheng *et al.* 2012). Among BTEX compounds, benzene is of the most concern because it is highly toxic and is a known carcinogen, and is listed as a US Environmental Protection Agency 'priority pollutant'. Several site specific surveys have documented a concentration range of 13–1,300 µg/L for benzene in drinking water after a period of water stagnation as a result of permeation through PB and PE pipes (Holsen *et al.* 1991). In a recent laboratory study by Mao *et al.* (2010), permeation by benzene through 1-inch diameter high density polyethylene (HDPE) pipe was found to be rapid, with a breakthrough time of 5 days for exposure to free product gasoline and 15 days for exposure to gasoline-saturated groundwater, respectively.

According to the theory of polymer permeability (Crank & Park 1968; Crank 1975; Comyn 1985), the permeation of organic contaminants through PE pipes may involve a three-step process: sorption consisting of contaminant molecules removal from contaminated soil and groundwater, diffusion of sorbed contaminant molecules through the amorphous area within pipe materials, and desorption of contaminant molecules from pipe materials to the pipe water. The three transport mechanisms are affected by various factors, such as: (i) molecular weight, size and shape of organic compounds; (ii) density, crystallinity, thickness, degree of crosslinking, chain rigidity and aging of polymer; (iii) chemical similarity between polymer and organic compounds; and (iv) initial bulk concentration of organic compounds (Sangam & Rowe 2001, 2005; Chao *et al.* 2006, 2007; Islam & Rowe 2009; Saquing *et al.* 2010; Whelton *et al.* 2010, 2011). For the PE pipe-contaminant system, these factors above can be quantified by some critical parameters such as solubility, diffusivity (diffusion coefficient), permeability, thickness of pipe wall, and contamination levels external to the pipe. Unfortunately, previous survey and laboratory studies have not provided sufficient information to assess the degree to which each process and parameter influence the permeation risks related to PE pipes. Therefore, a conceptually predictive model which incorporates these processes and parameters should be invaluable.

Mathematical modeling of the permeation of organic contaminants through plastic pipes has many potential applications. Conventionally, diffusion coefficient for a penetrant-polymer pair was determined by permeation experiments with the time-lag method (Crank 1975), which is based on the fact that the permeation rate of a penetrant that is brought into contact with a polymer sample becomes constant with time if the exposure concentration is kept a constant. If diffusion takes place in a hollow cylinder with inner and outer radii of a and b , respectively, the diffusion coefficients (D) can be estimated by (Crank 1975)

$$D = \frac{b^2 - a^2 + (a^2 + b^2) \ln(a/b)}{4T_L \ln(a/b)} \quad (1)$$

where T_L is the lag time, defined as the intersect with the time (t) axis of the straight line drawn through the plot of cumulative mass permeated per unit area $Q(t)$ data at

steady-state conditions are determined. The time-lag method only utilizes the steady-state permeation data and the accuracy of the determined diffusion coefficients strongly depends on the accuracy of the estimation of the lag time. Under some experimental conditions (such as the exposure to dilute contaminated aqueous solutions), it may be difficult to ascertain whether the steady-state permeation is achieved, mainly due to the slight change of the permeation flux with time and the random errors in the measurements. In this circumstance, the effectiveness of the time-lag method may need to be tested by other techniques such as numerical modeling simulation, which utilizes not only the steady-state permeation data, but also transient state data.

Estimation of the permeation parameters by mathematical modeling can help water utilities evaluate permeation risks for pipes with varied dimensions (sizes). In laboratory studies, small size pipes are typically used as they allow for easy installation and manipulation in the experimental apparatus. However, the permeation rates obtained from small size pipes may not be applicable for the estimation of risk for larger size pipes since the permeation rate strongly depends on the thickness of pipe wall. Moreover, water utilities are interested in the early stage of the permeation process, particularly the breakthrough time for a certain size pipe under a given contaminant level so that necessary activities can be taken within appropriate time. Theoretically, the permeation model can rapidly generate a complete permeation curve for any size pipe under any exposure condition if some permeation parameters (such as solubility and diffusion coefficient) are known.

Modeling studies may also be very useful in the prediction of permeation characteristics under field conditions. The constant exposure conditions in laboratory studies may not reflect actual permeation incidents in the real world where the exposure concentration may change with time, such as a groundwater plume traveling through the area where pipes are buried, or decay of environmental contaminants due to biodegradation. More specifically, it would be of interest to study the permeation characteristics if the contaminant plume is due to an instantaneous source or due to a continuous source with a constant input.

While mathematical modeling of the permeation process is useful, as discussed above, there is no study

reported in public literature that has utilized models to investigate the permeation process of organic contaminants through PE pipes. The objective of this study was to model the permeation process of benzene through HDPE pipes by using a numerical method. The developed permeation model takes account of the sorption, diffusion, and desorption processes. Permeation parameters (solubility, diffusivity, and permeability) were estimated by fitting the measured permeation data from Mao *et al.* (2010) to the model. Mao *et al.* (2010) investigated the permeation of BTEX compounds through PE pipes under certain simulated field conditions such as gasoline-contaminated groundwater with varied levels of contamination, and the permeation amounts of BTEX compounds through PE pipe were quantified for each specific testing condition. With the permeation parameters obtained, the model was then used to estimate the breakthrough time of benzene and its steady permeation flux into HDPE pipes of different diameters (sizes) under different exposure contamination levels. The permeation characteristics of benzene in HDPE pipes in some real-world conditions were finally simulated with varied time-dependent boundary conditions, by coupling the permeation model with subsurface transport

and degradation models. While a simplified model may not address very complex field conditions, this model captures the major mechanisms and factors that affect the permeation process in the field, and can be a useful screening tool for water utilities to estimate risk and expedite decision-making on permeation incidents.

METHODS

Experimental method and measurement

Measured permeation data reported by Mao *et al.* (2010) were used as a basis for this modeling study. Briefly, in the study by Mao *et al.* (2010), experiments were conducted using a pipe-bottle apparatus, consisting of a 1-L glass bottle with 25 mm (1 inch) diameter HDPE pipe mounted horizontally through holes drilled in the glass (Figure 1). HDPE pipes were exposed to silica sand saturated with gasoline-contaminated aqueous solutions with varied contamination levels (gasoline-saturated water, 50, and 10% of saturation). The silica sand and the aqueous solution were replaced each week with new sand and fresh aqueous

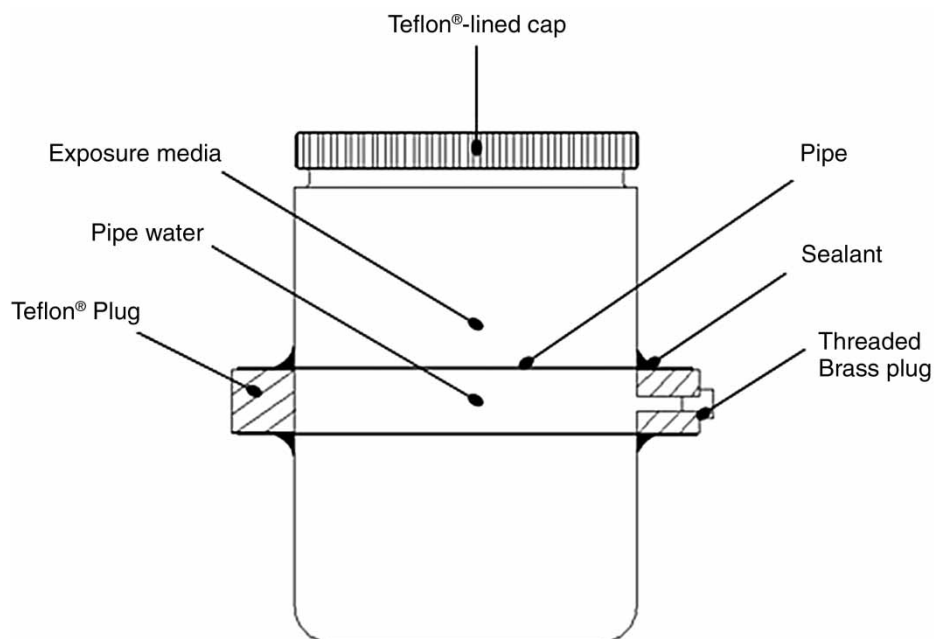


Figure 1 | Pipe-bottle apparatus.

gasoline solution to maintain relatively constant aqueous concentrations of BTEX in the bottle. BTEX concentrations in the soil pore water were periodically measured. Water inside the pipes was drained each week for BTEX analysis by using a gas chromatograph and the pipe water was replaced with fresh DI water after sampling. Only benzene was modeled since it is of the most concern among BTEX compounds. All the experiments were conducted at room temperature (23 ± 1.5 °C).

The experiments did not consider the effects of the hydrostatic pressure on permeation because both theoretical analyses (Selleck & Marinas 1991) and experimental results (Ong et al. 2008) indicated that the driving force for the permeation of organic compounds within pipe and gasket materials is the concentration gradient rather than the pressure gradient, and the influence of pressure on permeation is negligible at the pressure range commonly found in water distribution systems. Moreover, the permeation process may be temperature dependent, and temperature dependence of the diffusion coefficients can be described by the Arrhenius relationship (Saleem et al. 1989; Aminabhavi & Naik 1998). The soil temperature underground varies, depending on regional climate characteristics, soil characteristics (such as thermal conductivity) as well as the depth at which water mains and water services are buried. The experiments were conducted at room temperature, which may represent somewhat upper levels of soil temperatures underground where water mains and services are buried. Therefore, the diffusion coefficients obtained from the experiments may represent somewhat upper levels of diffusion coefficients in the field.

Permeation theory and modeling scheme

Figure 2 shows a schematic of the permeation process of benzene from the exterior environment (groundwater) to the water in the pipe. For the three-step permeation process described above, both sorption and desorption steps represent the partitioning of benzene between pipe materials and water. Since there are no solvency or swelling effects of benzene on PE materials, the partitioning process may proceed according to Henry's law

$$C_p^1 = SC_a^1 \quad (2)$$

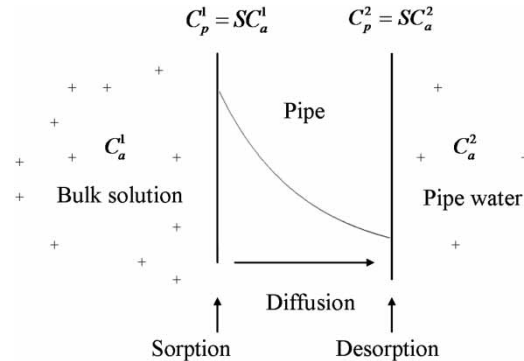


Figure 2 | Schematic of permeation of organic contaminants through PE pipes.

$$C_p^2 = SC_a^2 \quad (3)$$

where C_p^1 is the concentration of the contaminant on the outer wall of pipe in contact with the exterior environment (M/L^3); C_a^1 is the concentration of the contaminant in the exterior environment such as groundwater (M/L^3); C_p^2 is the concentration of the contaminant on the inner wall of pipe in contact with the water in the pipe (M/L^3); C_a^2 is the concentration of the contaminant in the water in the pipe (M/L^3); and S is the partitioning coefficient (sometimes called a solubility coefficient, dimensionless) and is a constant for a given contaminant, polymer, exposure/receiving medium and temperature of interest.

Diffusion of organic compounds in a cylinder can be described by Fick's law

$$\frac{\partial C_p}{\partial t} = \frac{1}{r} \frac{\partial}{\partial r} \left(rD \frac{\partial C_p}{\partial r} \right) \quad (4)$$

where C_p is the concentration of the contaminant in the PE material (M/L^3); D is the diffusion coefficient (L^2/T); and r is the cylindrical coordinate (L). The American Water Works Association standard dimension ratio DR (the ratio of the inside pipe diameter to the wall thickness) for the tested 25 mm (1 inch) standard inside dimension ratio (SIDR) 9 PE pipes was 9 (dimensionless). At this dimension ratio, the effect of pipe curvature on permeation can be safely ignored and the pipe configuration is reduced to that of a thin shell (Selleck & Marinas 1991). Therefore, the governing equation of Fick's law becomes

$$\frac{\partial C_p}{\partial t} = D \frac{\partial^2 C_p}{\partial x^2} \quad (5)$$

This simplification is applicable for all SIDR 9 and SIDR 7 pipes as modeled later in the section 'Estimation of breakthrough times and permeation fluxes for pipes with varied different diameters', as the ratio of the inside pipe diameter to the wall thickness for SIDR 9 pipes is 9 and for SIDR 7 pipes is 7, respectively.

For laboratory pipe-bottle experiments, the total quantity of contaminants diffusing into PE pipes as a function of time, Q_t (M/L^2) was measured under relatively strict conditions: (i) the concentration of the contaminant in the bulk solution (C_a^1) remained relatively constant; (ii) the initial concentration of the contaminant in the PE material was zero; and (iii) the inner concentration of the contaminant in the pipe water (C_a^2) was kept as low as possible by changing water frequently and assumed zero for the convenience of modeling. The initial and boundary conditions for modeling can be assumed to be where l is the wall thickness (L). Given a sufficient exposure time, the steady-state permeation flux [$M/(L^2/T)$] is given as

$$\begin{aligned} t < 0, \quad 0 \leq x \leq l, \quad C_p &= 0 \quad (\text{initial condition}) \\ t \geq 0, \quad x = 0, \quad C_p &= SC_a^1 \quad (\text{boundary condition for outer wall}) \\ t \geq 0, \quad x = l, \quad C_p &= 0 \quad (\text{boundary condition for inner wall}) \end{aligned} \quad (6)$$

$$F = DS \frac{(C_a^1 - C_a^2)}{l} = DS \frac{C_a^1}{l} = P \frac{C_a^1}{l} \quad (7)$$

where P [L^2/T] is defined as the permeability or permeation coefficient, which combines the components of diffusion coefficient and solubility coefficient. Essentially, P is a mass transfer coefficient that takes account of the sorption, diffusion, and desorption processes.

Determination of permeation parameters

The diffusion coefficient and solubility coefficient of benzene under three exposure conditions ($C_a^1 = 67.5 \pm 4.9$ mg/L, 31.2 ± 2.9 mg/L, and 6.0 ± 0.6 mg/L, respectively) were determined by fitting the measured permeation data for 1-inch SIDR 9 PE pipes to the permeation model. Explicit method was applied to estimate the cumulative permeation flux with time. The permeation flux into

the pipe at step j can be estimated by

$$F_j = D \times \frac{C_{m,j} - C_{m-1,j}}{dx} \times dt \quad (8)$$

where m is the number of equal subintervals (dx) of wall thickness (l), and dt is the subinterval time.

For the curve fitting process, the diffusion coefficients and the solubility coefficients determined by the time-lag method were used as the starting values. The time-lag method calculated the diffusion coefficients based on Equation (1) and then applied the calculated diffusion coefficients, measured steady-state permeation rates, exposure concentrations and pipe wall thickness to estimate the solubility coefficient based on Equation (7). The cumulative permeation flux was then estimated following the steps described above. The two parameters were adjusted through several trials until the observed data points matched the theoretical permeation curve. The

least-square method was used to test whether the 'best fit' was achieved. As the solubility coefficient is independent of the exposure concentration, the solubility coefficient was set as a constant for the three exposure conditions for an individual trial, and multiple trials were conducted to find the 'best' constant.

Estimation of breakthrough times and permeation fluxes for pipes with varied different diameters

Based on the thermodynamic view of the permeation process, the permeation of organic molecules through polymer materials is dependent on the chemical characteristics and concentration (activity) of the contaminant, the chemical characteristics of the polymer, and the interactions between the contaminant and the polymer. For the same pipe materials and the same exposure conditions, the diffusion

Table 1 | Dimensions of SIDR 7 and SIDR 9 series of HDPE pipes

Pipe type	Nominal O.D. ^a (mm) (inch)	O.D. ^a (inch)	I.D. ^b (inch)	Average wall thickness (inch)	O.D. ^a (cm)	I.D. ^b (cm)	Average wall thickness (cm)	
SIDR 7	20	3/4	1.070	0.824	0.123	2.718	2.093	0.312
	25	1	1.359	1.049	0.155	3.452	2.664	0.394
	32	1 (1/4)	1.785	1.380	0.202	4.534	3.505	0.514
	40	1 (1/2)	2.086	1.610	0.238	5.298	4.089	0.604
	50	2	2.675	2.067	0.304	6.795	5.250	0.772
SIDR 9	15	1/2	0.760	0.622	0.069	1.930	1.580	0.175
	20	3/4	1.018	0.824	0.097	2.586	2.093	0.246
	25	1	1.293	1.049	0.122	3.284	2.664	0.310
	40	1 (1/2)	1.918	1.610	0.154	4.872	4.089	0.391
	50	2	2.537	2.067	0.235	6.444	5.250	0.597

^aOuter diameter.^bInner diameter.

coefficient (D) and the solubility coefficient (S) obtained from 25 mm (1 inch) pipe SIDR 9 PE pipe experiments would remain valid for other pipe sizes. Permeation is then reduced to the effects of wall thickness of the pipe.

Model simulation was conducted for SIDR 9 and SIDR 7 series of commercial HDPE pipes (Table 1). Based on manufacturer's specification, SIDR 7 series pipes are of similar material to that of SIDR 9 series. The model simulation focused on the determination of two critical permeation parameters, the breakthrough time and the steady permeation flux of benzene. The breakthrough times of benzene were obtained by returning the simulation time once the arbitrary requirement (permeation flux $\leq 0.001 \mu\text{g}/\text{cm}^2$) was not met. The slopes of simulated permeation curves in later time (steady-state) periods were calculated to estimate the steady permeation flux for each size of pipe.

Prediction of permeation characteristics under time-dependent boundary conditions

The surface concentration at the outer wall generally varies with time in the field conditions. For this case, the boundary conditions for the outer wall (Equation (6)) can be modified to

$$t \geq 0, \quad x = 0, \quad C_p = SC_a^1(t) \quad (9)$$

where $C_a^1(t)$ is the concentration of the contaminant in the bulk solution at time (t). This study simulated three time-dependent boundary conditions: (i) degradation of benzene

with the first-order kinetics; (ii) a continuous source with a constant input of benzene; and (iii) a pulse source or a spill. Modeling simulations were conducted for a 25 mm (1 inch) SDIR 9 HDPE pipe exposed to benzene.

Case I: degradation with the first-order kinetics

The first-order degradation kinetics can be described by

$$C_a^1 = C_0 e^{-kt} \quad (10)$$

where C_0 is the initial concentration (M/L^3) and k is the first-order degradation constant (T^{-1}) of specific organic compound in an aquifer. For a specific compound, there is a large variation in degradation rate constant among different studies, mainly due to the difference in experimental conditions and aquifer characteristics. Here, a range of $0.005\text{--}0.02 \text{ day}^{-1}$ for benzene was selected on the basis of the *in situ* data reported by Nielsen *et al.* (1996). C_0 was arbitrarily set as $31.2 \text{ mg}/\text{L}$, an exposure concentration used in a laboratory study (Mao *et al.* 2010). It should be noted that this simulation was exclusively for the biodegradation of benzene external of the pipe and did not consider other physico-chemical processes that affect the boundary conditions.

Case II: continuous source with a constant input

The concentration, C , at some distance, L , from the source at concentration, C_0 , at time t , is given by the following

expression (Fetter 2000), where erfc is the complementary error function

$$C_a^1 = \frac{C_0}{2} \left[\text{erfc} \left(\frac{L - v_x t}{2\sqrt{D_L t}} \right) + \exp \left(\frac{v_x}{D_L} \right) \text{erfc} \left(\frac{L + v_x t}{2\sqrt{D_L t}} \right) \right] \quad (11)$$

where L is the flow path length (L), v_x is the average linear groundwater velocity (L/T), t is the times since release of the contaminant (T), and D_L is the longitudinal dispersion coefficient (L^2/T). This simulation assumed: $L = 10$ m (a drinking water pipe is located about 10 m from a leaking storage tank); $v_x = 0.05$ m/day, a typical value for groundwater movement in a sandy aquifer (Fetter 2000); and $D_L = 0.001$ – 0.05 m²/day (Fetter 2000). C_0 was set as 31.2 mg/L, being identical to that of Case I.

Case III: instantaneous source

The concentration of an instantaneous source of contaminant is best described using a Gaussian distribution curve. This variation of the advection-dispersion equation assumes a homogeneous, isotropic, and saturated porous medium; steady-state flow; and conditions where Darcy's law applies (Fetter 1999). The change of concentration in a pulse source with time in one dimension can be predicted by

$$C_a^1 = \frac{M}{(4\pi D_L t)^{1/2}} \exp \left[-\frac{(L - v_x t)^2}{4D_L t} \right] \quad (12)$$

where M is mass of contaminant per unit cross-sectional area (M/L^2). This simulation used the same values for parameters of L , v_x , and D_L , which were previously described in Case II. Based on Equation (12), M was set as 38 mg/m² to generate the external bulk concentrations which were comparable to the exposure concentrations used in the laboratory experiments, as reported in Mao et al. (2010).

As indicated above, the concentration at the outer wall which varies with time were given in the form of algebraic formula (Equations (10)–(12)). The data were substituted directly at each time step into the explicit scheme, i.e., at each time step the boundary condition for the outer wall was updated on the basis of the given algebraic formulas.

Scilab, a numerical computational package developed by INRIA and ENPC in Paris, France, was used to do all numerical analysis. Distributed with open source freely via

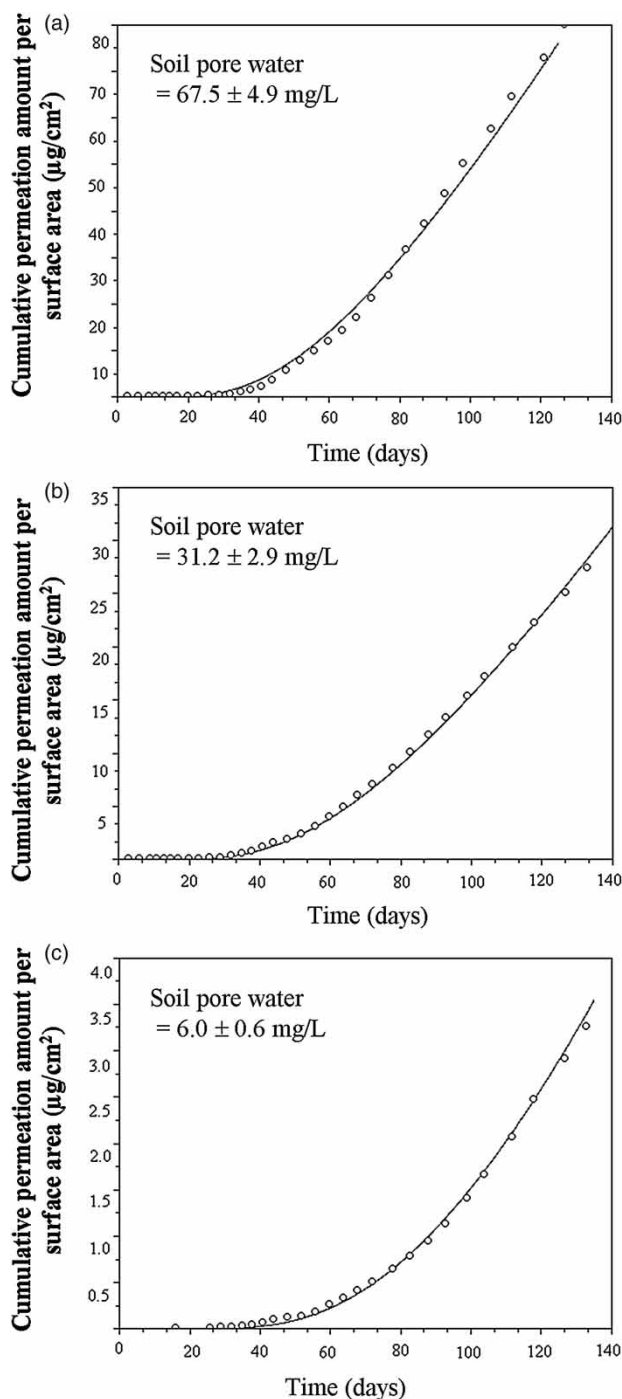
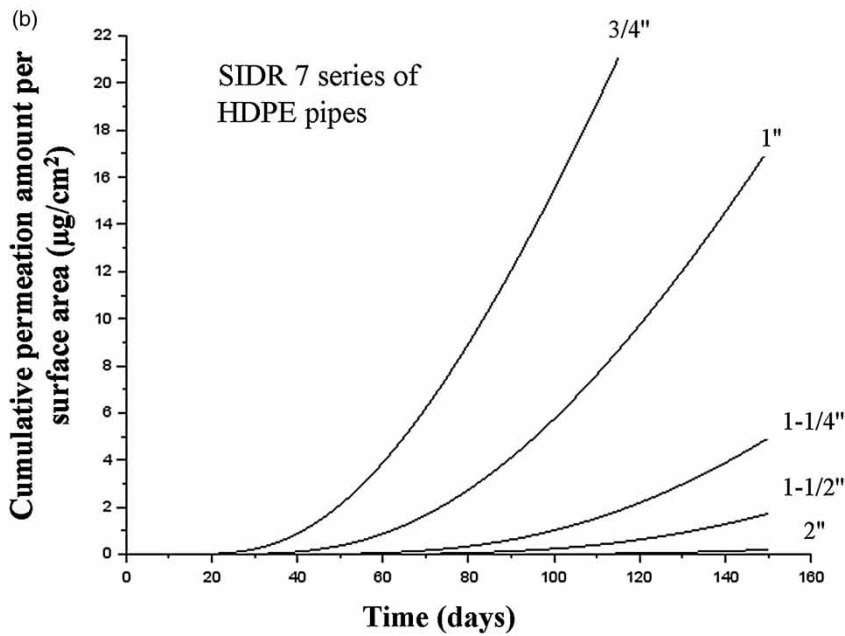
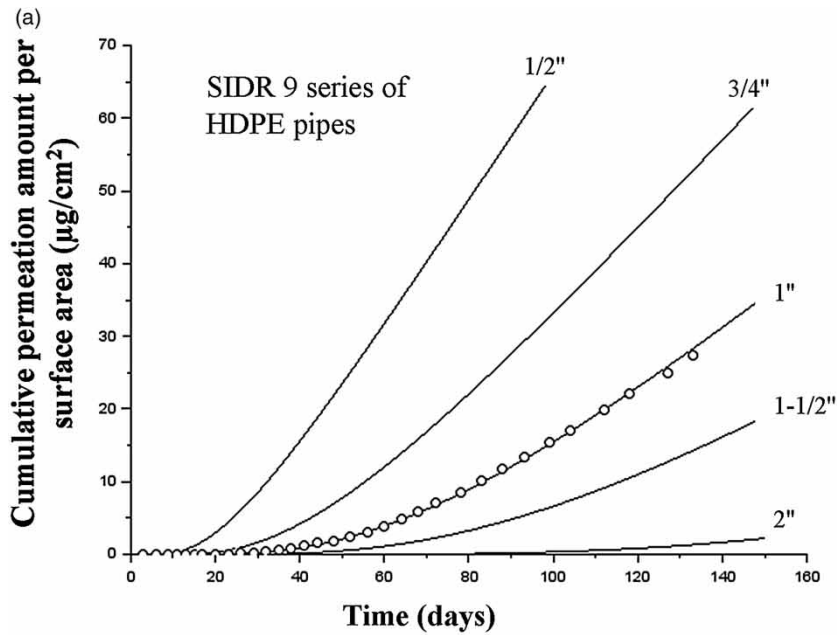


Figure 3 | Measured permeation data of benzene and curve fit data of permeation model: O, measured data; —, modeled curve.

the internet since 1994, *Scilab* is widely used as a powerful open computing environment for engineering and scientific applications (Bunks et al. 1999).

Table 2 | Permeation parameters of benzene determined by the numerical modeling method

Pipe type	Pipe thickness (mm)	C_1^0 (mg/L)	Diffusion coefficient ($\times 10^{-9}$ cm ² /s)	Solubility parameter	Steady-state permeation rate ($\mu\text{g}/(\text{cm}^2 \text{ day})$)
SIDR 9 1 inch (25 mm) pipe	3.1	67.5 ± 4.9	2.8	23.7	1.22
		31.2 ± 2.9	2.3	23.7	0.47
		6.0 ± 0.6	2.0	23.7	0.08

**Figure 4** | Simulated permeation curves of benzene for SIDR 9 and SIDR 7 series HDPE pipes (concentration of benzene in soil pore water: 31.2 ± 2.9 mg/L).

RESULTS AND DISCUSSION

Determination of permeation parameters

As shown in Figure 3, the measured data were well fitted by the permeation model. The predicted curve was able to capture the main characteristics of experimental data, i.e., there was a transient state from the time benzene first entered the pipe until the steady-state conditions were established. This simulation study confirmed the previous assumption that Fick's diffusion is the main mechanism for organic compounds to diffuse through PE pipe (Vonk 1985).

Table 2 summarizes the permeation parameters (diffusion coefficients, solubility coefficient, and steady-state permeation rates) of benzene determined by the numerical modeling method for different bulk exposure concentrations. It indicates that diffusion coefficients (D) as shown in Table 2 were concentration dependent and increased with an increase in bulk exposure concentration (C_a^1). This concentration effect may be attributed to increased mobility of polymer segments resulting from increases in the average free volume in the polymer caused by the presence of the diffusing contaminant (Crank & Park 1968). The relationship

between D and C_a^1 can be described by

$$D = D_0 e^{\alpha C_a^1} = 1.94 \times 10^{-9} e^{0.0055 C_a^1} \quad (R^2 = 1) \quad (13)$$

where D_0 is the diffusion coefficient in the limit as $C_a^1 \rightarrow 0$ (L^2/T), the characteristic diffusion coefficient for a specific polymer-penetrant pair; and α is the concentration-dependent constant. The exponential relationship between D and the bulk concentration has been found in the permeation of 1,2-dichloropropane through PB pipes (Park et al. 1991) and the permeation of *m*-xylene through HDPE geomembranes (Park et al. 1996). The diffusion coefficients determined from the model simulation were found to be lower than those determined from the time-lag method (Mao et al. 2010). For example, under an exposure concentration of 67.5 mg/L, the diffusion coefficient was 2.8×10^{-9} cm²/s from the model simulation and 3.6×10^{-9} cm²/s from the time-lag method, respectively. As previously discussed in the 'Introduction', the accuracy of the estimation of the lag time in the time-lag method may be challenged under certain experimental conditions, mainly due to slight changes of the permeation flux with time and the random errors in the analytical

Table 3 | Estimated breakthrough times and steady-state permeation rates of benzene for SIDR 7 and SIDR 9 series of HDPE pipes

Pipe	Concentration in soil pore water: 67.5 ± 4.9 mg/L		Concentration in soil pore water: 31.2 ± 2.9 mg/L		Concentration in soil pore water: 6.0 ± 0.6 mg/L	
	Breakthrough time ^a (days)	Steady-state permeation rate (µg/(cm ² day))	Breakthrough time ^a (days)	Steady-state permeation rate (µg/(cm ² day))	Breakthrough time ^a (days)	Steady-state permeation rate (µg/(cm ² day))
<i>SIDR 9</i>						
15 mm (1/2")	3.6	2.19	4.7	0.85	6.6	0.11
20 mm (3/4")	6.7	1.56	8.9	0.60	12.5	0.08
25 mm (1")	10.8	1.22	14.4	0.47	20.2	0.06
40 mm (1-1/2")	14.8	0.98	20.0	0.38	28.5	0.05
50 mm (2")	34	0.64	46.0	0.25	64.5	0.03
<i>SIDR 7</i>						
20 mm (3/4")	10.8	1.23	14.4	0.47	20.2	0.06
25 mm (1")	16.6	0.97	22.2	0.38	31.0	0.05
32 mm (1-1/4")	27.5	0.75	36.8	0.29	51.5	0.04
40 mm (1-1/2")	36.5	0.64	49.0	0.25	69.0	0.03
50 mm (2")	58	0.50	78.0	0.19	108.0	0.02

^aDefined as the exposure time when permeation flux ≤ 0.001 µg/cm² was not met.

measurements. If the experimental data misinterpret the steady-state permeation (i.e., the steady-state permeation is actually not achieved), the lag time is likely to be underestimated, resulting in the overestimation of the diffusion coefficient.

Using a constant solubility coefficient (S) of benzene led to a good fitting for all observed data. The value of S

determined in the present study (23.7) was very close to those obtained from two previous studies, 25.0 (Sangam & Rowe 2001) and 28.2 (Joo *et al.* 2004) on the permeation of benzene through HDPE geomembranes. An attempt was also done to directly apply the lag time-derived diffusion coefficients in the model simulations to estimate the solubility coefficient. The solubility coefficient was estimated as

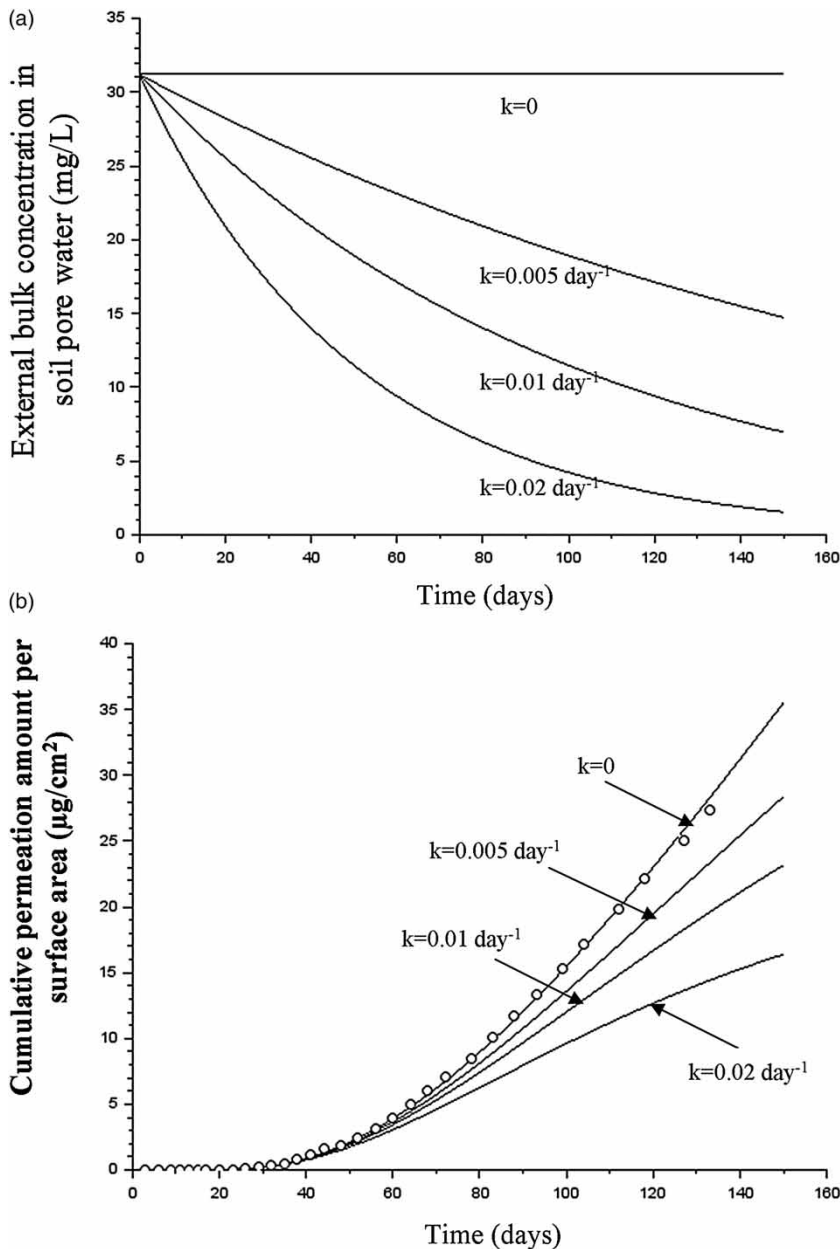


Figure 5 | (a) Change in external concentration with first-order degradation; (b) simulated permeation curves of benzene for 25 mm (1 inch) SIDR 9 HDPE pipe when the first-order degradation occurs.

17, lower than the solubility coefficient of 23.7 previously estimated. As presented above, the lag time-derived diffusion coefficients were higher than those determined from the permeation model simulations. Based on Equation (7), if a steady-state permeation rate is fixed, the solubility coefficient would decrease with the increase of the diffusion efficient.

Estimation of breakthrough times and permeation fluxes for pipes with different diameters

Simulated permeation curves were obtained for SIDR 9 and SIDR 7 series of HDPE pipes using the diffusion coefficients and solubility coefficient of benzene determined by the numerical modeling method (Figure 4). It is evident

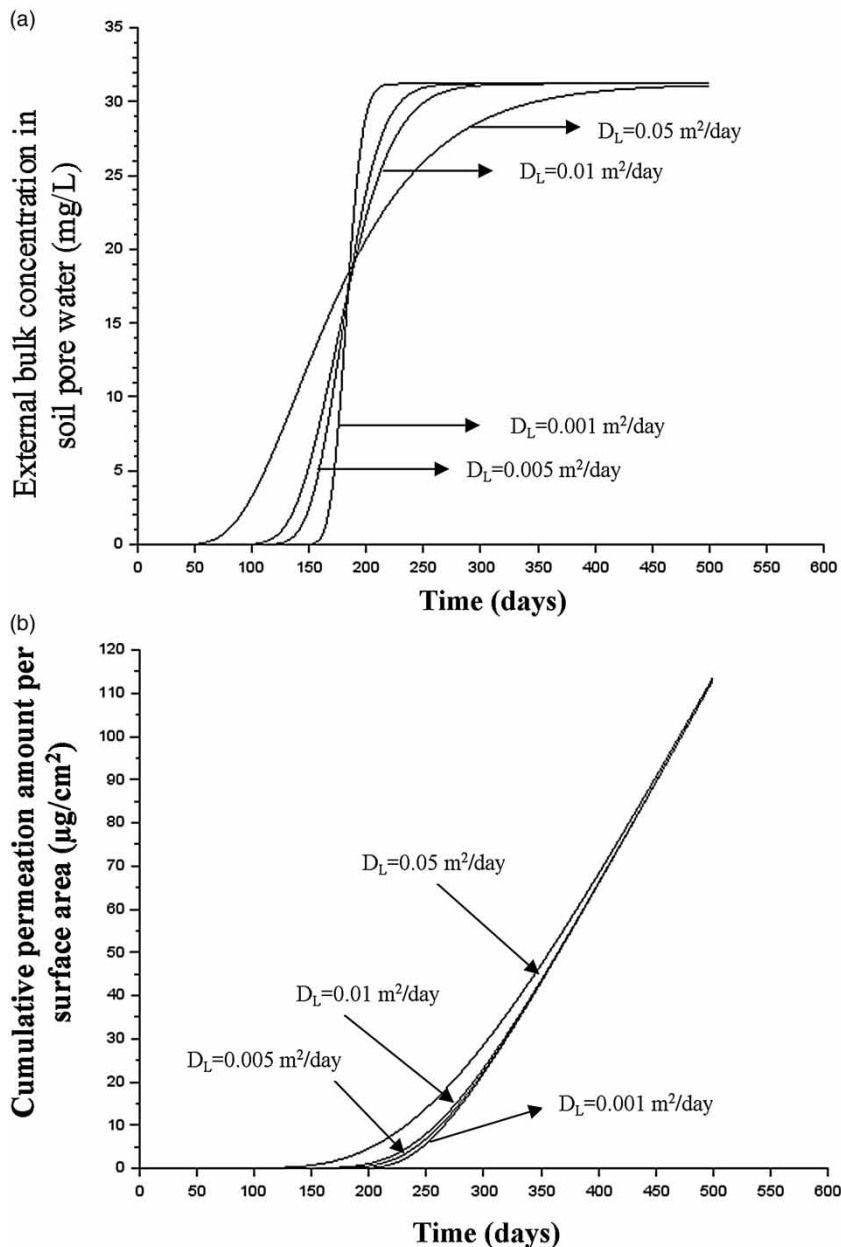


Figure 6 | (a) Concentration profile for a continuous source with a constant input; (b) simulated permeation curves of benzene for 25 mm (1 inch) SIDR 9 HDPE pipe that is buried in an aquifer with a continuous source releases benzene at 10 m away (average linear groundwater velocity $v_x = 0.056$ m/day).

from Figure 4 that small size pipes are more vulnerable to permeation than large diameter pipes for the same series of HDPE pipes. Under identical exposure conditions, the benzene breakthrough was longer and its permeation flux decreased with the increase in pipe diameters. The higher susceptibility of small size pipes to permeation is

supported by the findings of real permeation incidents, as reported in the study by Holsen *et al.* (1991), where all permeation incidents for service lines were associated with 25 mm (1 inch) or less diameter pipes. For an identical pipe dimension, SDR 7 series pipe is less permeable than SDR 9 series pipe. This is due to the

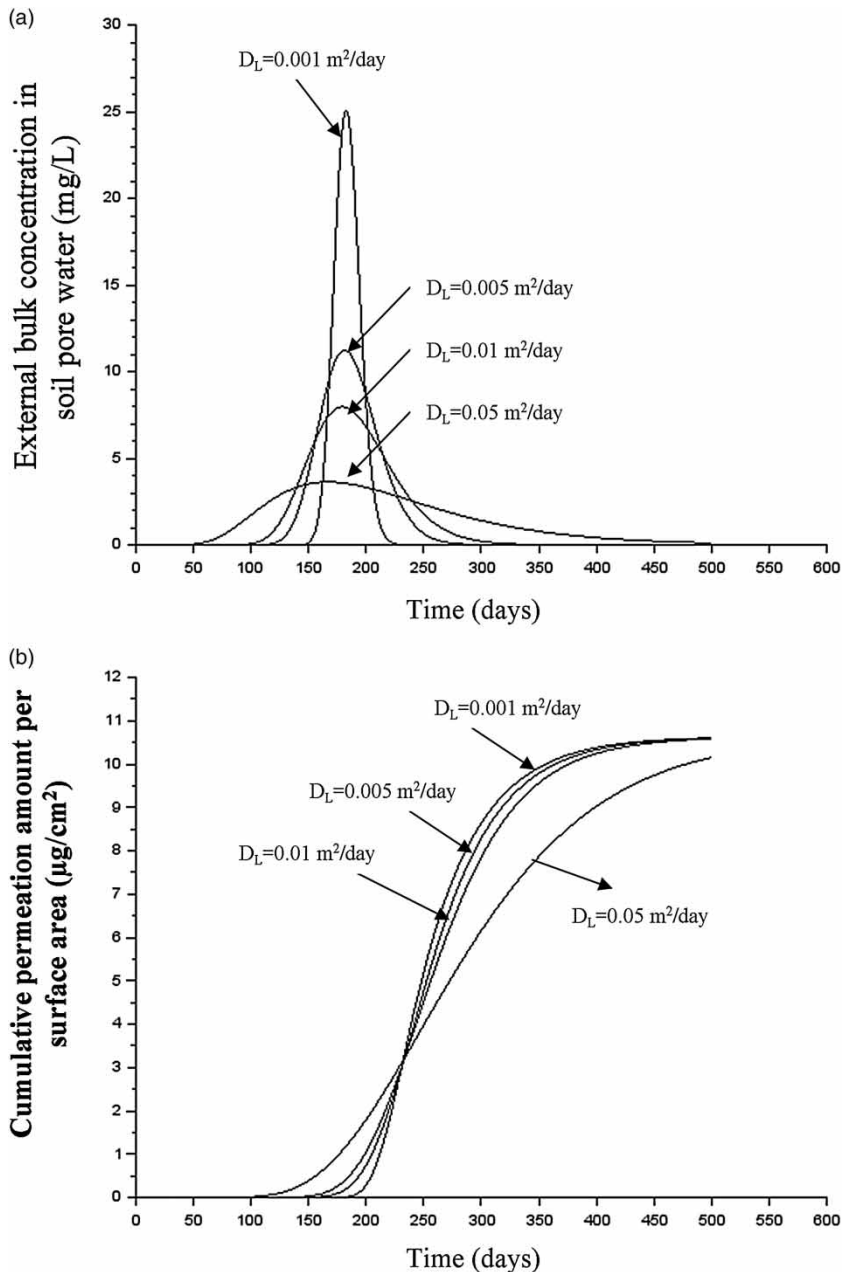


Figure 7 | (a) Concentration profile for a pulse source; (b) simulated permeation curves of benzene for 25 mm (1 inch) SDR 9 HDPE pipe that is buried in an aquifer where a pulse source releases benzene at 10 m away (average linear groundwater velocity $v_x = 0.056$ m/day; mass of benzene released: 38 mg/m²).

fact that SIDR 7 series (13.8 bar (200 psi) pressure rated) generally has a thicker wall than SIDR 9 pipe (11 bar (160 psi) pressure rated). Figure 4 also reveals that it takes a longer time to reach the steady-state permeation for larger diameter pipes and thus it is experimentally more difficult to use the time-lag method to determine the permeation parameters for 50 mm (2 inch) or larger diameter pipes.

Table 3 summarizes the breakthrough times and the steady-state permeation rates of benzene for various pipe diameters under three exposure conditions. As shown in Table 3, benzene rapidly permeates across 15 mm (1/2 inch) HDPE pipes within several days, while the breakthrough for 50 mm (2 inch) HDPE pipe lines occurred in one to a few months. The steady-state permeation rate of benzene for 15 mm (1/2 inch) pipe was more than three times higher than that for 50 mm (2 inch) diameter pipe.

Prediction of permeation behavior under time-dependent boundary conditions

Case I: degradation with the first-order kinetics

As shown in Figure 5, the permeation flux of benzene decreased with an increase of the first-order rate constant. That is not surprising, since large degradation rate constant indicates rapid degradation of organic compound surrounding pipes and the permeation flux is strongly dependent upon the external bulk concentration. For the three degradation conditions, the obtained permeation curves deviated from that of no decay condition at later time period and the rising slope became gentle with an increase in the first-order constant. However, the breakthrough of benzene occurred at the same time for the four conditions simulated, which implies that the degradation process is unable to prevent or retard the occurrence of permeation once the outer wall of pipes is contaminated and that breakthrough is only a function of the wall thickness.

Case II: continuous source with a constant input

If the flow length (the distance between the contaminant source and the target pipe) and the average linear groundwater velocity are constant, the concentrations of the

contaminant in the groundwater for a given time are strongly dependent upon the hydrodynamic dispersion coefficients (D_L), as shown in Figure 6. The benzene plume in the aquifer with the highest D_L first reached the target pipe, resulting in the rapid breakthrough of benzene at the pipe. On the contrary, the breakthrough time for lower D_L was retarded. Owing to the continuous and constant release of benzene, the external concentration of benzene surrounding pipes finally reached a constant value and consequently the four permeation curves with different dispersion coefficients were of the same magnitude, showing a linear increase with time, a characteristic of permeation curve for constant boundary conditions.

Case III: instantaneous source

An instantaneous source (such as a spill) yields a slug that grows with time as it moves down the groundwater flow path. In this case, D_L also significantly influences the contaminant concentration in groundwater and thus the permeation characteristics of contaminant through pipes, since it determines when the contaminant reaches pipes and how long the contaminant is in contact with pipes. As shown in Figure 7, the highest D_L led to the fastest breakthrough of benzene while the breakthrough was significantly retarded for lower D_L . In response to the sharp increase and decrease in the external concentration profile, the permeation curve at lower D_L was characterized by a dramatic increase in the permeation flux, followed by a rapid transition to the stationary phase.

CONCLUSION

A numerical modeling of the permeation of benzene through HDPE pipes was conducted. Based on the results of the numerical computation and analysis, the following conclusions can be drawn:

1. The measured data obtained from the pipe-bottle tests were well fitted using the permeation model based on a combination of equilibrium partition and classic Fick's diffusion. The results indicated that Fick's diffusion is the main mechanism for organic compounds to diffuse through PE pipe.

2. For the bulk concentrations between 6.0 and 67.5 mg/L in soil pore water, the concentration-dependent diffusion coefficients of benzene were found to range from 2.0×10^{-9} to 2.8×10^{-9} cm²/s while the solubility coefficient was determined to be 23.7.
3. For the same series of HDPE pipes, small diameter pipes are more vulnerable to permeation than large diameter pipes. Under identical exposure conditions, the breakthrough of organic contaminants was retarded and the corresponding permeation flux decreased with the increase of the pipe thickness.
4. Under field conditions, the permeation behavior of a specific organic compound is strongly dependent on the characteristics of contaminant source (instantaneous source or continuous source) and the properties of aquifer such as dispersion coefficients (D_L), which implicitly determine the effective contaminant concentration in groundwater that is available for permeation of the compound through pipe materials. Results of this modeling effort indicate that hydrocarbons such as benzene can be permeated through HDPE pipes into the drinking water and, in the event of a spill, the contaminated soils surrounding the HDPE pipes should be thoroughly remediated or the HDPE pipes replaced by pipes made of less permeable materials.

ACKNOWLEDGEMENTS

The authors thank the Water Research Foundation (formally AwwaRF) for its financial support and technical and administrative assistance. Comments and views detailed herein may not necessarily reflect the views of the Water Research Foundation, its officers, directors, affiliates, or agents.

REFERENCES

- Aminabhavi, T. M. & Naik, H. G. 1998 Chemical compatibility testing of geomembranes-sorption/desorption, diffusion and swelling phenomena. *Geotext. Geomembr.* **16** (6), 333–354.
- Berens, A. R. 1985 Prediction of organic chemical permeation through PVC pipe. *J. Am. Water Works Assoc.* **77** (11), 57–64.
- Bunks, C., Chancelier, J. P., Delebecque, F. & Goursat, M. 1999 *Engineering and Scientific Computing with Scilab*. Birkhäuser, Boston, MA, USA.
- Chao, K. P., Wang, P. & Lin, C. H. 2006 Estimation of diffusion coefficients and solubilities for organic solvents permeation through high-density polyethylene geomembrane. *J. Environ. Eng.* **132** (5), 519–526.
- Chao, K. P., Wang, P. & Wang, Y. T. 2007 Diffusion and solubility coefficients determined by permeation and immersion experiments for organic solvents in HDPE geomembrane. *J. Hazard. Mater.* **142** (1–2), 227–235.
- Cheng, C., Gaunt, J. A., Mao, F. & Ong, S. K. 2012 Permeation of gasoline through DI pipe gaskets in water mains. *J. Am. Water Works Assoc.* **104** (4), E271–E281.
- Comyn, J. 1985 *Polymer Permeability*. Elsevier Applied Science Publishers, Essex, UK.
- Crank, J. 1975 *The Mathematics of Diffusion*. Clarendon Press, Oxford, UK.
- Crank, J. & Park, G. S. 1968 *Diffusion in Polymers*. Academic Press, London, UK.
- Fetter, C. W. 1999 *Contaminant Hydrogeology*, Prentice-Hall, Upper Saddle River, NJ, USA.
- Fetter, C. W. 2000 *Applied Hydrogeology*, 4th edn. Prentice-Hall, Upper Saddle River, NJ, USA.
- Glaza, E. C. & Park, J. K. 1992 Permeation of organic contaminants through gasketed pipe joints. *J. Am. Water Works Assoc.* **84** (7), 92–100.
- Holsen, T. M., Paark, J. K., Jenkins, D. & Selleck, R. E. 1991 Contamination of potable water by permeation of plastic pipe. *J. Am. Water Works Assoc.* **83** (8), 53–56.
- Islam, M. Z. & Rowe, R. K. 2009 Permeation of BTEX through unaged and aged HDPE geomembranes. *J. Geotech. Geoenviron. Eng.* **135** (8), 1130–1140.
- Joo, J. C., Kim, J. Y. & Nam, K. 2004 Mass transfer of organic compounds in dilute aqueous solutions into high density polyethylene geomembranes. *J. Environ. Eng.* **130** (2), 175–183.
- Mao, F., Gaunt, J. A. & Ong, S. K. 2009 Permeation of organic contaminants through PVC pipes. *J. Am. Water Works Assoc.* **101** (5), 128–136.
- Mao, F., Gaunt, J. A., Cheng, C. L. & Ong, S. K. 2010 Permeation of BTEX compounds through HDPE pipes under simulated field conditions. *J. Am. Water Works Assoc.* **102** (3), 107–118.
- Mao, F., Gaunt, J. A., Cheng, C. L. & Ong, S. K. 2011a Microscopic visualization technique to predict the permeation of organic solvents through PVC pipes in water distribution system. *J. Environ. Eng.* **137** (2), 137–145.
- Mao, F., Gaunt, J. A., Ong, S. K. & Cheng, C. L. 2011b Permeation of petroleum-based hydrocarbons through PVC pipe joints with Rieber gasket systems. *J. Environ. Eng.* **137** (12), 1128–1135.
- Nielsen, P. H., Bjerg, P. L., Nielsen, P., Smith, P. & Christensen, T. H. 1996 *In situ* and laboratory determined first-order degradation constants of specific organic compounds in an aerobic aquifer. *Environ. Sci. Technol.* **30** (1), 31–37.
- Ong, S. K., Gaunt, J. A., Mao, F., Cheng, C. L., Agelet, L. E. & Hurlburgh, C. R. 2008 *Impact of Petroleum-Based*

- Hydrocarbons on PE/PVC Pipes and Pipe Gaskets*. AwwaRF, Denver, CO, USA.
- Park, J. K., Bontoux, L., Jenkins, D. & Selleck, R. E. 1991 Permeation of polybutylene pipe and gasket material by organic chemicals. *J. Am. Water Works Assoc.* **83** (10), 71–78.
- Park, J. K., Sakti, J. P. & Hoopes, J. A. 1996 Transport of organic compounds in thermoplastic geomembranes. I: Mathematical model. *J. Environ. Eng.* **122** (9), 800–806.
- Saleem, M., Asfour, A. A., De Kee, D. & Harison, B. 1989 Diffusion of organic penetrant through low density polyethylene (LDPE) films: effect of size and shape of the penetrant molecules. *J. Appl. Polym. Sci.* **37** (3), 617–625.
- Sangam, H. P. & Rowe, R. K. 2001 Migration of dilute aqueous organic pollutants through HDPE geomembranes. *Geotext. Geomembr.* **19** (6), 329–357.
- Sangam, H. P. & Rowe, R. K. 2005 Effect of surface fluorination on diffusion through a high-density polyethylene geomembrane. *J. Geotech. Geoenviron. Eng.* **131** (6), 694–704.
- Saquin, J. M., Saquin, C. D., Knappe, D. U. & Barlaz, M. A. 2010 Impact of plastics on fate and transport of organic contaminants in landfills. *Environ. Sci. Technol.* **44** (16), 6396–6402.
- Selleck, R. E. & Marinas, B. J. 1991 Analyzing the permeation of organic chemicals through plastic pipes. *J. Am. Water Works Assoc.* **83** (8), 92–97.
- Thompson, C. & Jenkins, D. 1987 *Review of Water Industry Plastic Pipe Practices*. AwwaRF, Denver, CO, USA.
- US EPA 2002 Permeation and leaching: technical information review. Available from: www.epa.gov/safewater/disinfection/tcr/pdfs/whitepaper_tcr_permation-leaching.pdf.
- Vonk, M. W. 1985 *Permeation of Organic Compounds through Pipe Materials*, Pub. No. 85. KIWA, Neuwegein, the Netherlands.
- Whelton, A. J., Dietrich, A. M. & Gallagher, D. L. 2010 Contaminant diffusion, solubility, and material property differences between HDPE and PEX potable water pipes. *J. Environ. Eng.* **136** (2), 227–237.
- Whelton, A. J., Dietrich, A. M. & Gallagher, D. L. 2011 Impact of chlorinated water exposure on contaminant transport and surface and bulk properties of high-density polyethylene and cross-linked polyethylene potable water pipes. *J. Environ. Eng.* **137** (7), 559–568.

First received 26 July 2014; accepted in revised form 25 January 2015. Available online 13 March 2015